Swansea University
Prifysgol Abertawe

ZCCE

Characterising the shape of and material properties of hidden conducting targets in metal detection

P.D. Ledger

Zienkiewicz Centre for Computational Engineering, College of Engineering,

Swansea University, UK

W.R.B. Lionheart

School of Mathematics,

The University of Manchester, UK

Supported by EPSRC Grant EP/K00428X/1.

Applications of finding hidden objects

In many practical applications the goal is locate and identify hidden conducting objects from field measurements:

Security Screening

Archeological Searches

UXO and mine clearence

Medical Imaging

Non-destructive testing

Food Safety

This requires solving an **inverse problem**, which is generally more challenging compared to the corresponding **direct problem**. The applications and techniques involve different regimes of electromagnetism.

Why are inverse problems challenging?

- Typically ill-posed (lacks one or more conditions for well-posedness) e.g.
  - possible lack of existence;
  - possible lack of uniqueness;
  - possible lack of stability.
- In practice only limited noisy measurement data is available

Practical engineering solutions to Inverse problems are often posed as minimisation problems e.g.

$$\min_{\boldsymbol{p}} \|\boldsymbol{d} - \boldsymbol{F}(\boldsymbol{p})\|^2 + \|\boldsymbol{R}(\boldsymbol{p}))\|^2$$

In the above

- $\boldsymbol{d}$ represents some *measured* data;
- $\boldsymbol{F}(\boldsymbol{p})$ represents the *direct* or *forward* problem, parameterised by model parameters $\boldsymbol{p}$;
- $\boldsymbol{R}(\boldsymbol{p})$ is some regularisation which may be added to help overcome the ill-posedness.

But there are computational challenges of dimensionality, local minima and choosing $\boldsymbol{R}$.

Basic idea of object characterisation using polarizability tensors

When an object is introduced in to a background field u_0 it will perturb it resulting in u_α, e.g. in plane wave scattering of an object

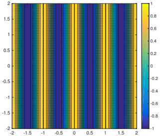

u_0

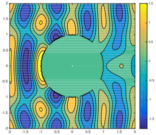

u_α

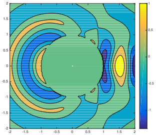

$u_\alpha - u_0$

We are interested in finding expressions of the form

$$(u_\alpha - u_0)(\boldsymbol{x}) = f(\mathcal{T}, u_0(\boldsymbol{z}), G(\boldsymbol{x}, \boldsymbol{z})) + R$$

to use as the **direct problem**.

- $\boldsymbol{z}$ is the position of the centre of the object.
- $\mathcal{T}$ is a position independent polarizability tensor describing the shape and material of the object
- R is some small quantifiable remainder.
- $G(\boldsymbol{x}, \boldsymbol{z})$ is an appropriate (free space) Green's function.
- Also has connections with the construction of cloaking of objects.

Electrical impedance tomography

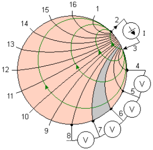

Given measurements of boundary voltages $u|_{\partial\Omega}$ and external currents $I(\boldsymbol{x}) := \hat{\boldsymbol{n}} \cdot \sigma_\alpha \nabla u|_{\partial\Omega}$ we want to **find the conductivity distribution** $\sigma_\alpha(\boldsymbol{x})$.

The Maxwell system simplifies since $\omega\mu|\sigma_\alpha|\alpha \ll 1$. Introducing $\boldsymbol{E} = \nabla u_\alpha$ where u_α solves

$$\begin{aligned} \nabla \cdot \sigma_\alpha \nabla u_\alpha &= 0 && \text{in } \Omega \subset \mathbb{R}^3 \\ \hat{\boldsymbol{n}} \cdot \sigma_\alpha \nabla u_\alpha &= I && \text{on } \partial\Omega \\ \int_{\partial\Omega} I \mathrm{d}\boldsymbol{x} &= 0 \end{aligned}$$

The case of $\alpha = 0$, ie u_0, corresponds to the case of a known constant background σ_0.

Electrical impedance tomography

The effect of introducing a small object D with conductivity σ_* in a background field u_0 is like introducing a dipole at its centre z

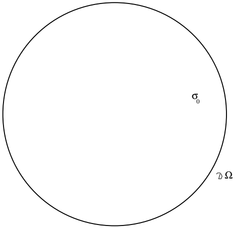

Background problem

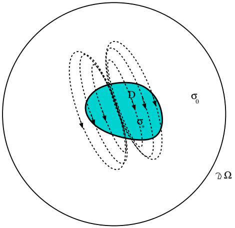

Perturbed problem

For a small single inclusion $D := \alpha B + z$ with contrast $c := \frac{\sigma_*}{\sigma_0}$ Ammari and Kang (2007) show that for a related unbounded problem

$$(u_\alpha - u_0)(\boldsymbol{x}) = \nabla_x \left(G(\boldsymbol{x}, \boldsymbol{z}) \right) \cdot \left(\mathcal{T}(c) \, \nabla_z u_0(\boldsymbol{z}) \right) + O\left(\alpha^4\right)$$

as $\alpha \to 0$ where $G(\boldsymbol{x}, \boldsymbol{z}) := 1/(4\pi|\boldsymbol{x} - \boldsymbol{z}|)$. Results are also available for the bounded EIT case (Cedio-Fengya, Moskow, Vogeliuis (1998), Ammari and Kang (2007))

Computing the Póyla–Szegö tensor

The coefficients of the tensor are

$$\mathcal{T}(c)_{ij} = \alpha^3 \left((c-1)|B|\delta_{ij} + (c-1)^2 \int_\Gamma \hat{\boldsymbol{n}} \cdot \nabla \phi_i|^- \xi_j \mathrm{d}\boldsymbol{\xi} \right),$$

where ϕ_i, $i = 1, 2, 3$, satisfies the transmission problem

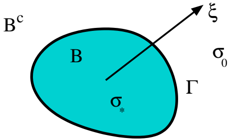

$$\begin{aligned} \nabla^2 \phi_i &= 0 && \text{in } B \cup B^c, \\ [\phi_i]_\Gamma = 0, \qquad [\hat{\boldsymbol{n}} \cdot \sigma \nabla \phi_i]_\Gamma &= \sigma_0 \hat{\boldsymbol{n}} \cdot \nabla \xi_i && \text{on } \Gamma, \\ \phi_i &\to 0 && \text{as } |\boldsymbol{\xi}| \to \infty. \end{aligned}$$

- $\mathcal{T}$ is a real symmetric tensor **defined by** 6 **coefficients**;
- $\mathcal{T}$ can be diagonalised and an equivalent best fitting ellipsoid found that has the same $\mathcal{T}$ as the object D;
- $\mathcal{T}$ contains both **shape and material contrast information**;
- Determining the coefficients of $\mathcal{T}$ and the location z from $u|_{\partial\Omega}$ and I offers possibilities for **low-cost identification of inclusions**;

Computing the Póyla–Szegö tensor

The coefficients of the tensor are

$$\mathcal{T}(c)_{ij} = \alpha^3 \left((c-1)|B|\delta_{ij} + (c-1)^2 \int_\Gamma \hat{\boldsymbol{n}} \cdot \nabla\phi_i|^- \xi_j \mathrm{d}\boldsymbol{\xi} \right),$$

where ϕ_i, $i = 1, 2, 3$, satisfies the transmission problem

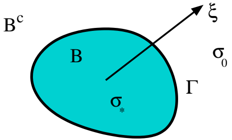

$$\begin{aligned} & & \nabla^2\phi_i &= 0 & &\text{in } B \cup B^c, \\ [\phi_i]_\Gamma &= 0, & [\hat{\boldsymbol{n}} \cdot \sigma\nabla\phi_i]_\Gamma &= \sigma_0 \hat{\boldsymbol{n}} \cdot \nabla\xi_i & &\text{on } \Gamma, \\ & & \phi_i &\to 0 & &\text{as } |\boldsymbol{\xi}| \to \infty. \end{aligned}$$

- $\mathcal{T}$ is a real symmetric tensor **defined by** 6 **coefficients**;
- $\mathcal{T}$ can be diagonalised and an equivalent best fitting ellipsoid found that has the same $\mathcal{T}$ as the object D;
- $\mathcal{T}$ contains both **shape and material contrast information**;
- Determining the coefficients of $\mathcal{T}$ and the location z from $u|_{\partial\Omega}$ and I offers possibilities for **low-cost identification of inclusions**;

Electromagnetic scattering

For known analytic incident fields $\boldsymbol{E}^{in} = \boldsymbol{E}_0$, $\boldsymbol{H}^{in} = \boldsymbol{H}_0$ and measured scattered fields $\boldsymbol{E}^{sc} := \boldsymbol{E}_\alpha - \boldsymbol{E}^{in}$, $\boldsymbol{H}^{sc} := \boldsymbol{H}_\alpha - \boldsymbol{H}^{in}$ we want to infer information about the shape of the shape of scatterer D and the contrasts ϵ_*/ϵ_0 and μ/μ_0.

For wave number $\kappa := \omega\sqrt{\epsilon_0\mu_0}$ the fields satisfy the (scaled) Maxwell system

$$\begin{aligned} \nabla \times \boldsymbol{E}_\alpha &= \mathrm{i}\kappa\mu_\alpha^r \boldsymbol{H}_\alpha, \qquad & \nabla \times \boldsymbol{H}_\alpha &= -\mathrm{i}\epsilon_\alpha^r \kappa \boldsymbol{E}_\alpha \qquad & \text{in } \mathbb{R}^3, \\ \nabla \cdot \epsilon_\alpha^r \boldsymbol{E}_\alpha &= 0 & \nabla \cdot \mu_\alpha^r \boldsymbol{H}_\alpha &= 0 & \text{in } \mathbb{R}^3, \end{aligned}$$

For smooth, simply connected objects $D := \alpha B + z$ (PDL, WRBL 2015a)

$$\begin{aligned} (\boldsymbol{E}_\alpha - \boldsymbol{E}^{in})(\boldsymbol{x})_i = &\alpha^3 \kappa^2 \mathcal{G}^\kappa(\boldsymbol{x}, \boldsymbol{z})_{ij} \left(\mathcal{T}\left(\frac{\epsilon_*}{\epsilon_0} \right) \right)_{jk} \boldsymbol{E}^{in}(\boldsymbol{z})_k + \\ &+ \alpha^3 \mathrm{i}\kappa (\nabla_x \times \mathcal{G}^\kappa(\boldsymbol{x}, \boldsymbol{z}))_{ij} \left(\mathcal{T}\left(\frac{\mu_*}{\mu_0} \right) \right)_{jk} \boldsymbol{H}^{in}(\boldsymbol{z})_k + O(\Gamma^4), \end{aligned}$$

as $\Gamma := \max(\kappa\alpha, \alpha/r) \to 0$, with $r := |\boldsymbol{x} - \boldsymbol{z}|$

$$\mathcal{G}^\kappa(\boldsymbol{x}, \boldsymbol{z})_{ij} := G^\kappa((\boldsymbol{x}, \boldsymbol{z})\delta_{ij} + \frac{1}{\kappa^2}(D_x^2 G^\kappa(\boldsymbol{x}, \boldsymbol{z}))_{ij} \qquad G^\kappa = \frac{e^{\mathrm{i}\kappa|\boldsymbol{x} - \boldsymbol{z}|}}{4\pi|\boldsymbol{x} - \boldsymbol{z}|}$$

with a similar result for $\boldsymbol{H}_\alpha - \boldsymbol{H}^{in}$.

Electromagnetic scattering

For known analytic incident fields $\boldsymbol{E}^{in} = \boldsymbol{E}_0$, $\boldsymbol{H}^{in} = \boldsymbol{H}_0$ and measured scattered fields $\boldsymbol{E}^{sc} := \boldsymbol{E}_\alpha - \boldsymbol{E}^{in}$, $\boldsymbol{H}^{sc} := \boldsymbol{H}_\alpha - \boldsymbol{H}^{in}$ we want to infer information about the shape of the shape of scatterer D and the contrasts ϵ_*/ϵ_0 and μ/μ_0.

For wave number $\kappa := \omega\sqrt{\epsilon_0\mu_0}$ the fields satisfy the (scaled) Maxwell system

$$\begin{aligned} \nabla \times \boldsymbol{E}_\alpha &= \mathrm{i}\kappa\mu_\alpha^r \boldsymbol{H}_\alpha, \qquad \nabla \times \boldsymbol{H}_\alpha = -\mathrm{i}\epsilon_\alpha^r \kappa \boldsymbol{E}_\alpha && \text{in } \mathbb{R}^3, \\ \nabla \cdot \epsilon_\alpha^r \boldsymbol{E}_\alpha &= 0 \qquad \nabla \cdot \mu_\alpha^r \boldsymbol{H}_\alpha = 0 && \text{in } \mathbb{R}^3, \end{aligned}$$

For smooth, simply connected objects $D := \alpha B + \boldsymbol{z}$ (PDL, WRBL 2015a)

$$\begin{aligned} (\boldsymbol{E}_\alpha - \boldsymbol{E}^{in})(\boldsymbol{x})_i =& \alpha^3 \kappa^2 \mathcal{G}^\kappa(\boldsymbol{x},\boldsymbol{z})_{ij} \left(\mathcal{T}\left(\frac{\epsilon_*}{\epsilon_0}\right)\right)_{jk} \boldsymbol{E}^{in}(\boldsymbol{z})_k + \\ & + \alpha^3 \mathrm{i}\kappa (\nabla_x \times \mathcal{G}^\kappa(\boldsymbol{x},\boldsymbol{z}))_{ij} \left(\mathcal{T}\left(\frac{\mu_*}{\mu_0}\right)\right)_{jk} \boldsymbol{H}^{in}(\boldsymbol{z})_k + O(\Gamma^4), \end{aligned}$$

as $\Gamma := \max(\kappa\alpha, \alpha/r) \to 0$, with $r := |\boldsymbol{x} - \boldsymbol{z}|$

$$\mathcal{G}^\kappa(\boldsymbol{x},\boldsymbol{z})_{ij} := G^\kappa((\boldsymbol{x},\boldsymbol{z})\delta_{ij} + \frac{1}{\kappa^2}(\boldsymbol{D}_x^2 G^\kappa(\boldsymbol{x},\boldsymbol{z}))_{ij} \qquad G^\kappa = \frac{e^{\mathrm{i}\kappa|\boldsymbol{x}-\boldsymbol{z}|}}{4\pi|\boldsymbol{x}-\boldsymbol{z}|}$$

with a similar result for $\boldsymbol{H}_\alpha - \boldsymbol{H}^{in}$.

For large r and fixed α this agrees with the far field term obtained by Kleinman (*et al.* (1982)

$$\frac{\alpha^3\kappa}{r}\left(\hat{\boldsymbol{r}}\times\hat{\boldsymbol{r}}\times\left(\mathcal{T}\left(\frac{\epsilon_*}{\epsilon_0}\right)\boldsymbol{E}^{in}(\boldsymbol{z})\right)+\hat{\boldsymbol{r}}\times\left(\mathcal{T}\left(\frac{\mu_*}{\mu_0}\right)\boldsymbol{H}^{in}(\boldsymbol{z})\right)\right)+O(\kappa^2)$$

as $\kappa\to 0$. On the other hand, fixing κ, r then is of the same form of Ammari, Volkov (2005) for small objects.

$$\begin{aligned}(\boldsymbol{E}_\alpha-\boldsymbol{E}^{in})(\boldsymbol{x})_i =&\alpha^3\kappa^2\mathcal{G}^\kappa(\boldsymbol{x},\boldsymbol{z})_{ij}\left(\mathcal{T}\left(\frac{\epsilon_*}{\epsilon_0}\right)\right)_{jk}\boldsymbol{E}^{in}(\boldsymbol{z})_k+\\ &+\alpha^3\mathrm{i}\kappa(\nabla_x\times\mathcal{G}^\kappa(\boldsymbol{x},\boldsymbol{z}))_{ij}\left(\mathcal{T}\left(\frac{\mu_*}{\mu_0}\right)\right)_{jk}\boldsymbol{H}^{in}(\boldsymbol{z})_k+O(\alpha^4),\end{aligned}$$

as $\alpha\to 0$

GPR one possible application but not metal detection.

We have an analogous result for objects with $(\epsilon_*+\mathrm{i}\sigma_*/\omega)/\epsilon_0$ but this is for fixed κ and thus does not apply to low frequencies.

Describing the response from metal detectors

Eddy current approximation.

$\sqrt{\epsilon_* \mu_*}\alpha\omega \ll 1, \epsilon_*\omega/\sigma_* \ll 1$(rigorous justification involves the topology of the object).

Current source $\boldsymbol{J}_0$ at $\boldsymbol{w}$ idealsied as a dipole with moment $\boldsymbol{m}$ generates $\boldsymbol{H}_0(\boldsymbol{x}) = \boldsymbol{D}_x^2 G(\boldsymbol{x},\boldsymbol{w})\boldsymbol{m}$.

From measurements of $(\boldsymbol{H}_\alpha - \boldsymbol{H}_0)(\boldsymbol{x})$ we want to find information about an object's shape and μ_*/μ_0, σ_*.

The interaction fields satisfy

$$\begin{aligned} \nabla \times \boldsymbol{E}_\alpha &= \mathrm{i}\omega\mu_\alpha \boldsymbol{H}_\alpha, & \nabla \times \boldsymbol{H}_\alpha &= \sigma_\alpha \boldsymbol{E}_\alpha + \boldsymbol{J}_0 & &\text{in } \mathbb{R}^3, \\ \nabla \cdot \boldsymbol{E}_\alpha &= 0 & \nabla \cdot \mu_\alpha \boldsymbol{H}_\alpha &= 0 & &\text{in } \mathbb{R}^3. \end{aligned}$$

Polarizability tensors for the eddy current problem

For the case where $\nu = 2\alpha^2/s^2 = O(1)$, ($s = \sqrt{2/(\omega\mu_*\sigma_*)}$ and $\mu_r = \mu_*/\mu_0$) Ammari, Chen, Chen, Garnier and Volkov (2013) have shown that

$$(\boldsymbol{H}_\alpha - \boldsymbol{H}_0)(\boldsymbol{x})_j = \boldsymbol{D}^2 G(\boldsymbol{x},\boldsymbol{z})_{\ell m}\mathcal{M}_{\ell m j i}\boldsymbol{H}_0(\boldsymbol{z})_i + O(\alpha^4)$$

as $\alpha \to 0$ for fixed $\boldsymbol{x}$ away from $\boldsymbol{z}$

In the above $\mathcal{M}$ is a **new rank 4 tensor**, which depends on the shape of the object, μ_r and σ_*.

Note the response is not characterised by a suitably parameterised $\mathcal{T}$.

But, **electrical engineers predict that the response from a conducting object form a single measure-excitor coil pair** as

$$\text{Voltage signal} \approx \boldsymbol{m}_j^{ms}(\boldsymbol{H}_\alpha - \boldsymbol{H}_0)(\boldsymbol{x})_j \approx \boldsymbol{H}_0^{ms}(\boldsymbol{z})_j \overset{\smile}{\mathcal{M}}_{ji}\boldsymbol{H}_0(\boldsymbol{z})_i \ (= \boldsymbol{D}^2 G(\boldsymbol{x},\boldsymbol{z})_{jk}\boldsymbol{m}_k^{ms}\overset{\smile}{\mathcal{M}}_{ji}\boldsymbol{H}_0(\boldsymbol{z})_i)$$

They fit coefficients to rank 2 tensor $\overset{\smile}{\mathcal{M}}$ but they don't have an explicit formula .

Polarizability tensors for the eddy current problem

For the case where $\nu = 2\alpha^2/s^2 = O(1)$, ($s = \sqrt{2/(\omega\mu_*\sigma_*)}$ and $\mu_r = \mu_*/\mu_0$) Ammari, Chen, Chen, Garnier and Volkov (2013) have shown that

$$(\boldsymbol{H}_\alpha - \boldsymbol{H}_0)(\boldsymbol{x})_j = \boldsymbol{D}^2 G(\boldsymbol{x},\boldsymbol{z})_{\ell m} \mathcal{M}_{\ell m j i} \boldsymbol{H}_0(\boldsymbol{z})_i + O(\alpha^4)$$

as $\alpha \to 0$ for fixed $\boldsymbol{x}$ away from $\boldsymbol{z}$

In the above $\mathcal{M}$ is a **new rank 4 tensor**, which depends on the shape of the object, μ_r and σ_*.

Note the response is not characterised by a suitably parameterised $\mathcal{T}$.

But, **electrical engineers predict that the response from a conducting object form a single measure-excitor coil pair** as

$$\text{Voltage signal} \approx \boldsymbol{m}_j^{ms} (\boldsymbol{H}_\alpha - \boldsymbol{H}_0)(\boldsymbol{x})_j \approx \boldsymbol{H}_0^{ms}(\boldsymbol{z})_j \breve{\breve{\mathcal{M}}}_{ji} \boldsymbol{H}_0(\boldsymbol{z})_i \ (= \boldsymbol{D}^2 G(\boldsymbol{x},\boldsymbol{z})_{jk} \boldsymbol{m}_k^{ms} \breve{\breve{\mathcal{M}}}_{ji} \boldsymbol{H}_0(\boldsymbol{z})_i)$$

They fit coefficients to rank 2 tensor $\breve{\breve{\mathcal{M}}}$ but they don't have an explicit formula .

Computing $\mathcal{M}$

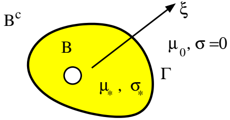

$$\mathcal{M}_{\ell mji} := \mathcal{P}_{\ell mji} + \delta_{\ell j}\delta_{mk}\mathcal{N}_{ki}$$

$$\mathcal{P}_{\ell mji} := \beta \hat{\boldsymbol{e}}_j \cdot \left(\hat{\boldsymbol{e}}_\ell \times \int_B \xi_m (\boldsymbol{\theta}_i + \hat{\boldsymbol{e}}_i \times \boldsymbol{\xi}) \mathrm{d}\boldsymbol{\xi} \right),$$

$$\mathcal{N}_{ki} := \alpha^3 \left(1 - \frac{\mu_0}{\mu_*}\right) \int_B \left(\hat{\boldsymbol{e}}_k \cdot \hat{\boldsymbol{e}}_i + \frac{1}{2} \hat{\boldsymbol{e}}_k \cdot \nabla \times \boldsymbol{\theta}_i \right) \mathrm{d}\boldsymbol{\xi}.$$

$\beta = -\frac{\mathrm{i}\nu\alpha^3}{2}$ and $\boldsymbol{\theta}_i$, $i = 1, 2, 3$, is the solution to

$$\nabla \times \mu^{-1} \nabla \times \boldsymbol{\theta}_i - \mathrm{i}\omega\sigma\alpha^2 \boldsymbol{\theta}_i = \mathrm{i}\omega\sigma\alpha^2 \hat{\boldsymbol{e}}_i \times \boldsymbol{\xi} \qquad \text{in } B \cup B^c,$$

$$\nabla \cdot \boldsymbol{\theta}_i = 0 \qquad \text{in } B^c,$$

$$[\boldsymbol{\theta}_i \times \hat{\boldsymbol{n}}]_\Gamma = \boldsymbol{0}, \qquad \left[\mu^{-1} \nabla \times \boldsymbol{\theta}_i \times \hat{\boldsymbol{n}}\right]_\Gamma = -2 \left[\mu^{-1}\right]_\Gamma \hat{\boldsymbol{e}}_i \times \hat{\boldsymbol{n}} \qquad \text{on } \Gamma,$$

$$\boldsymbol{\theta}_i(\boldsymbol{\xi}) = O(|\boldsymbol{\xi}|^{-1}) \qquad \text{as } |\boldsymbol{\xi}| \to \infty,$$

Reduction to a Rank 2 Tensor

For orthonormal coordinates we have shown (PDL & WRBL 2015) that

$$(\boldsymbol{H}_\alpha - \boldsymbol{H}_0)(\boldsymbol{x})_j = \boldsymbol{D}^2_{\boldsymbol{x}} G(\boldsymbol{x},\boldsymbol{z})_{jm} \breve{\breve{\breve{\mathcal{M}}}}_{mi} \boldsymbol{H}_0(\boldsymbol{z})_i + O(\alpha^4),$$

where $\breve{\breve{\breve{\mathcal{M}}}}_{mi} = -\check{\mathcal{C}}_{mi} + \mathcal{N}_{mi}$ are the coefficients of a complex symmetric rank 2 tensor.

Proof:
The skew symmetry of $\mathcal{P}$, $\mathcal{P}_{\ell m j i} = -\mathcal{P}_{j m \ell i}$ allows us to write

$$\mathcal{C}_{nsi} = \frac{1}{2}\varepsilon_{sjl}\mathcal{P}_{\ell nji} \qquad \mathcal{P}_{\ell mji} = \varepsilon_{j\ell s}\mathcal{C}_{msi}$$

where $\mathcal{C}$ is a rank 3 tensor density.

The rank 3 tensor density has coefficients which satisfy $\mathcal{C}_{msi} = -\mathcal{C}_{smi}$ and so

$$\check{\mathcal{C}}_{mi} := \frac{\beta}{2}\hat{\boldsymbol{e}}_m \cdot \int_B \boldsymbol{\xi} \times (\boldsymbol{\theta}_i + \hat{\boldsymbol{e}}_i \times \boldsymbol{\xi}) \mathrm{d}\boldsymbol{\xi} = \frac{1}{4}\varepsilon_{mns}\varepsilon_{sjl}\mathcal{P}_{\ell nji} = \frac{1}{2}\varepsilon_{mns}\mathcal{C}_{nsi}, \qquad \mathcal{C}_{msi} = \varepsilon_{msk}\check{\mathcal{C}}_{kl}$$

Combining this with the fact that $\boldsymbol{D}^2 G(\boldsymbol{x},\boldsymbol{z})_{\ell m} = \boldsymbol{D}^2 G(\boldsymbol{x},\boldsymbol{z})_{m\ell}$ and $\boldsymbol{D}^2 G(\boldsymbol{x},\boldsymbol{z})_{\ell\ell} = 0$ completes the proof.

- Predicts the voltage in terms of a complex symmetric rank 2 tensor $\breve{\breve{\breve{\mathcal{M}}}}$ with **6 complex coefficients**. **Agrees with engineering prediction** and provides an explicit formula for the Magnetic Polarizability tensor that **allow us to explore object characteristics**

Reduction to a Rank 2 Tensor

For orthonormal coordinates we have shown (PDL & WRBL 2015) that

$$(\boldsymbol{H}_\alpha - \boldsymbol{H}_0)(\boldsymbol{x})_j = \boldsymbol{D}^2_{\boldsymbol{x}} G(\boldsymbol{x},\boldsymbol{z})_{jm} \overset{\smile\smile}{\mathcal{M}}_{mi} \boldsymbol{H}_0(\boldsymbol{z})_i + O(\alpha^4),$$

where $\overset{\smile\smile}{\mathcal{M}}_{mi} = -\check{\mathcal{C}}_{mi} + \mathcal{N}_{mi}$ are the coefficients of a complex symmetric rank 2 tensor.

Proof:
The skew symmetry of $\mathcal{P}$, $\mathcal{P}_{\ell mji} = -\mathcal{P}_{jm\ell i}$ allows us to write

$$\mathcal{C}_{nsi} = \frac{1}{2}\varepsilon_{sjl}\mathcal{P}_{\ell nji} \qquad \mathcal{P}_{\ell mji} = \varepsilon_{j\ell s}\mathcal{C}_{msi}$$

where $\mathcal{C}$ is a rank 3 tensor density.

The rank 3 tensor density has coefficients which satisfy $\mathcal{C}_{msi} = -\mathcal{C}_{smi}$ and so

$$\check{\mathcal{C}}_{mi} := \frac{\beta}{2}\hat{\boldsymbol{e}}_m \cdot \int_B \boldsymbol{\xi} \times (\boldsymbol{\theta}_i + \hat{\boldsymbol{e}}_i \times \boldsymbol{\xi})\mathrm{d}\boldsymbol{\xi} = \frac{1}{4}\varepsilon_{mns}\varepsilon_{sjl}\mathcal{P}_{\ell nji} = \frac{1}{2}\varepsilon_{mns}\mathcal{C}_{nsi}, \qquad \mathcal{C}_{msi} = \varepsilon_{msk}\check{\mathcal{C}}_{kl}$$

Combining this with the fact that $\boldsymbol{D}^2 G(\boldsymbol{x},\boldsymbol{z})_{\ell m} = \boldsymbol{D}^2 G(\boldsymbol{x},\boldsymbol{z})_{m\ell}$ and $\boldsymbol{D}^2 G(\boldsymbol{x},\boldsymbol{z})_{\ell\ell} = 0$ completes the proof.

- Predicts the voltage in terms of a complex symmetric rank 2 tensor $\overset{\smile\smile}{\mathcal{M}}$ with **6 complex coefficients**. **Agrees with engineering prediction** and provides an explicit formula for the Magnetic Polarizability tensor that **allow us to explore object characteristics**

Further reductions in the number of independent coefficients

If an object has mirror or rotation symmetries the coefficients of the tensor must remain invariant under this transformation.

- Under the action of an orthogonal matrix $\mathcal{R}$

$$\breve{\breve{\mathcal{M}}}'_{ij} = \mathcal{R}_{i\ell}\mathcal{R}_{jm}\breve{\breve{\mathcal{M}}}_{\ell m}.$$

We can deduce the number of independent coefficients:

Object				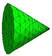	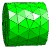		
$\breve{\breve{\mathcal{M}}}$	1	1	3	2	2	2	3

Computational treatment of transmission problem

Follow PDL, Zaglmayr (2010), truncate at a finite distance from the object, introduce the domain $\Omega = B \cup \tilde{B}^c$ and solve for $\boldsymbol{\vartheta}_i = \overline{\boldsymbol{\theta}}_i$, $i = 1, 2, 3$:

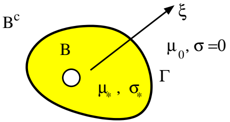

$$
\begin{aligned}
\nabla \times \mu_r^{-1} \nabla \times \boldsymbol{\vartheta}_i + \mathrm{i}\mu_0\omega\sigma_* \alpha^2 \boldsymbol{\vartheta}_i &= -\mathrm{i}\mu_0\omega\sigma_*\alpha^2 \hat{\boldsymbol{e}}_i \times \boldsymbol{\xi} && \text{in } B,\\
\nabla \times \nabla \times \boldsymbol{\vartheta}_i + \tau \boldsymbol{\vartheta}_i &= \mathbf{0} && \text{in } \tilde{B}^c,\\
[\boldsymbol{\theta}_i \times \hat{\boldsymbol{n}}]_\Gamma &= \mathbf{0} && \text{on } \Gamma,\\
\left[\tilde{\mu}_r^{-1} \nabla \times \boldsymbol{\vartheta}_i \times \hat{\boldsymbol{n}}\right]_\Gamma &= -2\left[\tilde{\mu}_r^{-1}\right]_\Gamma \hat{\boldsymbol{e}}_i \times \hat{\boldsymbol{n}} && \text{on } \Gamma,\\
\nabla \times \boldsymbol{\vartheta}_i \times \hat{\boldsymbol{n}} &= \mathbf{0} && \text{on } \partial\Omega,
\end{aligned}
$$

where $\|\boldsymbol{\vartheta}_i - \overline{\boldsymbol{\theta}}_i\|_{H(\mathrm{curl})} \leqslant C\tau$, C independent of the small perturbation parameter τ.
Weak form: find $\boldsymbol{\vartheta}_i^\tau \in \boldsymbol{H}(\mathrm{curl}, \Omega)$ such that

$$
(\tilde{\mu}_r^{-1} \nabla \times \boldsymbol{\vartheta}_i^\tau, \nabla \times \boldsymbol{v})_\Omega + (\tilde{\kappa} \boldsymbol{\vartheta}_i^\tau, \boldsymbol{v})_\Omega =
$$
$$
-(\mathrm{i}\mu_0\omega\sigma\alpha^2 \hat{\boldsymbol{e}}_i \times \boldsymbol{\xi}, \boldsymbol{v})_B - 2\int_\Gamma [\tilde{\mu}_r^{-1}] \hat{\boldsymbol{e}}_i \times \hat{\boldsymbol{n}} \cdot \overline{\boldsymbol{v}} \mathrm{d}\boldsymbol{\xi},
$$

for all $\boldsymbol{v} \in \boldsymbol{H}(\mathrm{curl}, \Omega)$ where $(\cdot, \cdot)_\Omega$ is the L_2 inner product and

$$
\tilde{\kappa} = \begin{cases} \mathrm{i}\mu_0\omega\sigma\alpha^2 & \text{in } B \\ \tau & \text{in } \tilde{B}^c \end{cases} \qquad \tilde{\mu}_r = \begin{cases} \mu_r & \text{in } B \\ 1 & \text{in } \tilde{B}^c \end{cases} .
$$

Verification with known analytical results for $\check{\check{\mathcal{M}}}$

Spherical object $\sigma_* = 5.96e7$S/m, $\mu_* = 1.5\mu_0$, $\omega = 133.5$rad/s, $\alpha = 0.01$m

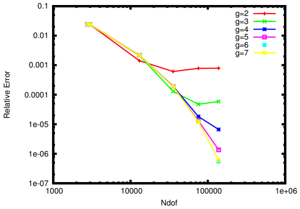

hp FEM convergence

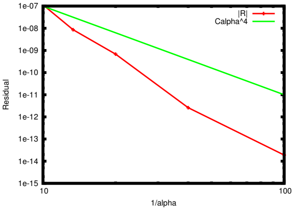

Decay of remainder

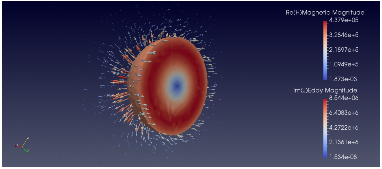

Re$(\nabla \times \boldsymbol{\theta}_1)$, $|$Im$(\omega\sigma\boldsymbol{\theta}_1)|$

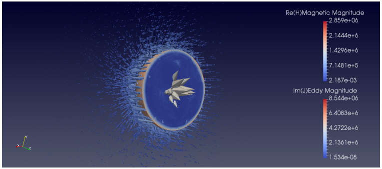

and now with $\omega = 133.5 \times 10^3$rad/s

Limiting cases of $\check{\check{\mathcal{M}}}$

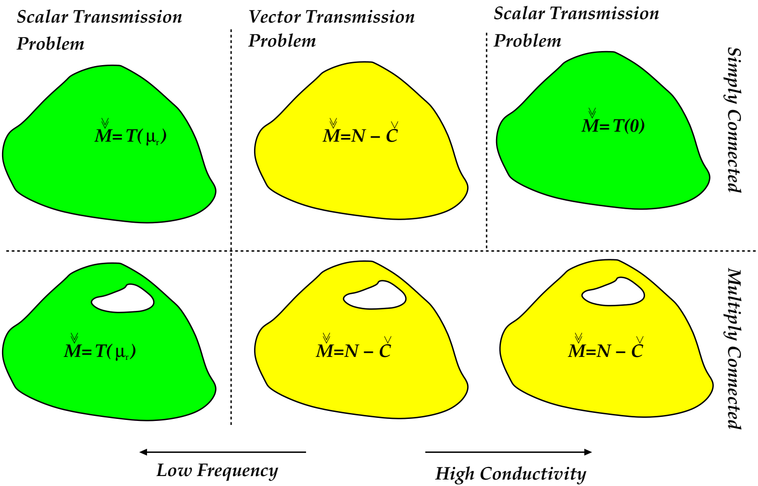

Similar results can be obtained for small σ_* and large ω, but they need to be interpreted in terms of the limit of the eddy current model. (PDL, WRBL (2016)).

Low Frequency and High Conductivity Response

Independent of Betti number $\beta_1(B)$ for an object with conductivity σ_* and relative permeability $\mu_r = \mu_*/\mu_0$, (PDL, WRBL 2016)

$$\underset{\approx}{\mathcal{M}}_{ij} = \mathcal{T}_{ij}(\mu_r) + O(\omega) \qquad \text{as } \omega \to 0$$

For an object with $\beta_1(B) = 0$, μ_r and fixed ω then

$$\underset{\approx}{\mathcal{M}}_{ij} = \mathcal{T}_{ij}(0) + O(1/\sqrt{\sigma_*}) \qquad \text{as } \sigma_* \to \infty$$

where

$$\mathcal{T}_{ij}(0) = \alpha^3 \left(|B|\delta_{ij} - \int_\Gamma \hat{\boldsymbol{n}}^- \cdot \hat{\boldsymbol{e}}_i \phi_j \mathrm{d}\boldsymbol{\xi} \right) \qquad \text{Magnetic tensor for a PEC}$$

$$\begin{aligned} \nabla^2 \phi_j &= 0 && \text{in } B^c \\ \hat{\boldsymbol{n}} \cdot \nabla \phi_j &= \hat{\boldsymbol{n}} \cdot \nabla \xi_j && \text{on } \Gamma \\ \phi_j &\to 0 && \text{as } |\boldsymbol{\xi}| \to \infty \end{aligned}$$

- The **Betti number does not play a role in objects at low frequencies, but does play a role in high conductivities**.

Low Frequency and High Conductivity Response

Independent of Betti number $\beta_1(B)$ for an object with conductivity σ_* and relative permeability $\mu_r = \mu_*/\mu_0$, (PDL, WRBL 2016)

$$\overset{\approx}{\mathcal{M}}_{ij} = \mathcal{T}_{ij}(\mu_r) + O(\omega) \qquad \text{as } \omega \to 0$$

For an object with $\beta_1(B) = 0$, μ_r and fixed ω then

$$\overset{\approx}{\mathcal{M}}_{ij} = \mathcal{T}_{ij}(0) + O(1/\sqrt{\sigma_*}) \qquad \text{as } \sigma_* \to \infty$$

where

$$\mathcal{T}_{ij}(0) = \alpha^3 \left(|B|\delta_{ij} - \int_\Gamma \hat{\boldsymbol{n}}^- \cdot \hat{\boldsymbol{e}}_i \phi_j \mathrm{d}\boldsymbol{\xi} \right) \qquad \text{Magnetic tensor for a PEC}$$

$$\begin{aligned} \nabla^2 \phi_j &= 0 && \text{in } B^c \\ \hat{\boldsymbol{n}} \cdot \nabla \phi_j &= \hat{\boldsymbol{n}} \cdot \nabla \xi_j && \text{on } \Gamma \\ \phi_j &\to 0 && \text{as } |\boldsymbol{\xi}| \to \infty \end{aligned}$$

- The **Betti number does not play a role in objects at low frequencies, but does play a role in high conductivities**.

Frequency response of a conducting (magnetic) spheroid

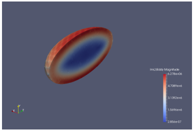

$$\sigma_* = 1.5 \times 10^7 \text{S/m}$$
$$\mu_* = \mu_0$$
$$\beta_0(B) = 1,$$
$$\beta_1(B) = \beta_2(B) = 0$$

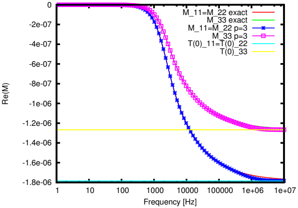

$\mathrm{Re}(\breve{\breve{\mathcal{M}}})$

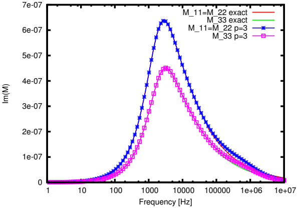

$\mathrm{Im}(\breve{\breve{\mathcal{M}}})$

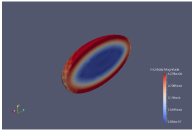

$$\sigma_* = 1.5 \times 10^7 \text{S/m}$$
$$\mu_* = 1.5\mu_0$$
$$\beta_0(B) = 1,$$
$$\beta_1(B) = \beta_2(B) = 0$$

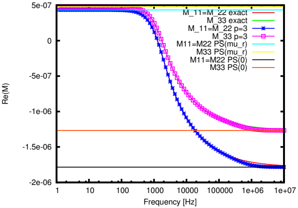

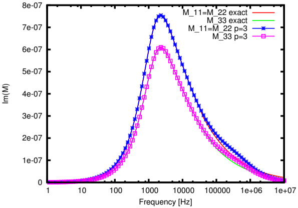

Comparing analytical solution for conducting permeable spheroid, $p = 3$ elements on a mesh of 14 579 tetrahedra and limiting Póyla–Szegö tensor coefficents

Frequency response of multiply connected objects

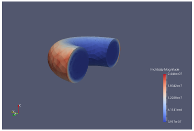

$$\sigma_* = 5.96 \times 10^7 \text{S/m}$$
$$\mu_* = 1.5\mu_0$$
$$\beta_0(B) = \beta_1(B) = 1,$$
$$\beta_2(B) = 0$$

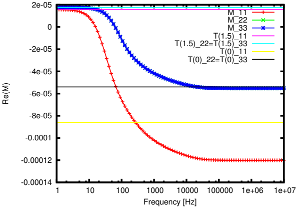

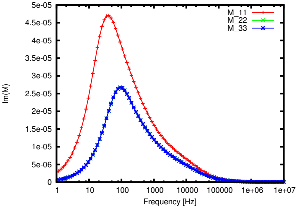

Re($\widetilde{\widetilde{\mathcal{M}}}$) Im($\widetilde{\widetilde{\mathcal{M}}}$)

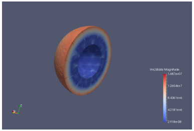

$$\sigma_* = 5.96 \times 10^7 \text{S/m}$$
$$\mu_* = 1.5\mu_0$$
$$\beta_0(B) = \beta_2(B) = 1,$$
$$\beta_1(B) = 0$$

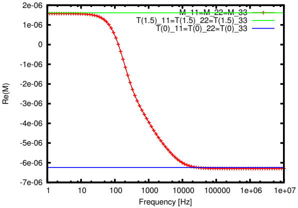

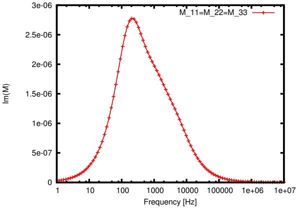

$p = 2$ elements on meshes of 29 882, 6 873 tetrahedra respectively, comparison with limiting Póyla–Szegö tensor coefficents

Realistic Remington .222 shell casing test case

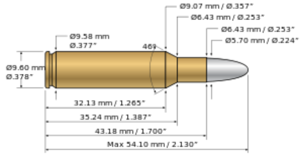

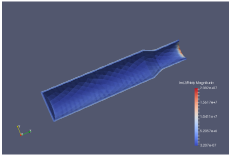

z axis parallel to barrel

- Only shell casing considered with $\mu_* = \mu_0$ and $\sigma_* = 1.5 \times 10^7$S/m.
- Rotational and reflection symmetries imply $\breve{\breve{\mathcal{M}}}$ is diagonal with coefficients $\breve{\breve{\mathcal{M}}}_{11} = \breve{\breve{\mathcal{M}}}_{22}$ and $\breve{\breve{\mathcal{M}}}_{33}$.

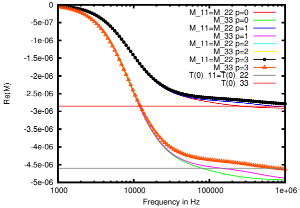

$\mathrm{Re}(\breve{\breve{\mathcal{M}}})$

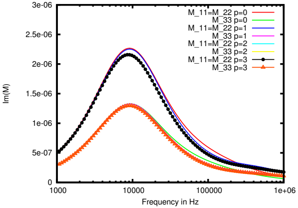

$\mathrm{Im}(\breve{\breve{\mathcal{M}}})$

First steps with Bayesian inversion

Recall at the start we stated the inverse problem as the minimisation problem.

$$\min_{\boldsymbol{p}} \|\boldsymbol{d} - \boldsymbol{F}(\boldsymbol{p})\|^2 + \|\boldsymbol{R}(\boldsymbol{p}))\|^2$$

Polarization tensors offer a low–cost way of describing the forward problem $\boldsymbol{F}(\boldsymbol{p})$, where $\boldsymbol{p} := \{\breve{\breve{\mathcal{M}}}_{11}, \breve{\breve{\mathcal{M}}}_{22}, \breve{\breve{\mathcal{M}}}_{33}, \breve{\breve{\mathcal{M}}}_{12}, \breve{\breve{\mathcal{M}}}_{13}, \breve{\breve{\mathcal{M}}}_{23}\}$, say.

The Bayesian approach can be thought of as being natural when statistical information about the noise is available:

- Likelihood density $\pi(\boldsymbol{d}|\boldsymbol{p}) \sim \exp\{-\frac{1}{2}(\boldsymbol{F}(\boldsymbol{p}) - \boldsymbol{d})_i C_{ij}^{-1}(\boldsymbol{F}(\boldsymbol{p}) - \boldsymbol{d})_j\}$ if $\boldsymbol{e} \sim \mathcal{N}(0, C)$.
- Prior probability distribution $\pi(\boldsymbol{p}) \sim \exp\{-\frac{1}{2}\boldsymbol{p}_i D_{ij}^{-1}\boldsymbol{p}_j\}$ for a regularising prior with $\boldsymbol{p} \sim \mathcal{N}(0, D)$
- Bayes formula then gives the posterior as a probability distribution

$$\begin{aligned}\pi(\boldsymbol{p}|\boldsymbol{d}) \sim& \pi(\boldsymbol{d}|\boldsymbol{p})\pi(\boldsymbol{p}) \\ \sim& \exp\left\{-\frac{1}{2}(\boldsymbol{F}(\boldsymbol{p}) - \boldsymbol{d})_i C_{ij}^{-1}(\boldsymbol{F}(\boldsymbol{p}) - \boldsymbol{d})_j - \frac{1}{2}\boldsymbol{p}_i D_{ij}^{-1}\boldsymbol{p}_j\right\}\end{aligned}$$

(written for simplicity for the real case)

Exploring the probability distribution

Notice that for different trial solutions $\boldsymbol{u}$, $\pi(\boldsymbol{p}|\boldsymbol{d})$ gives us the probability of $\boldsymbol{p}$ given $\boldsymbol{d}$

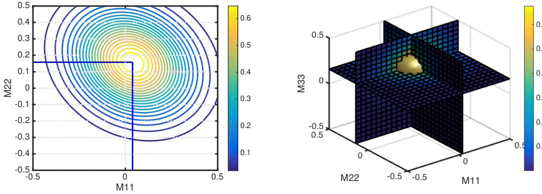

We can interogate the distribution using conditional mean (CM), maximum a–posterior (MAP) estimates, which for Gaussian distributions become

$$\boldsymbol{u}_{CM} = \boldsymbol{p}_{MAP} = \min \mathcal{F}(\boldsymbol{p}) = \min \frac{1}{2}\left(\|\boldsymbol{F}(\boldsymbol{p}) - \boldsymbol{d}\|_V^2 + \lambda\|\boldsymbol{p}\|_W^2\right)$$

$$= \min \frac{1}{2}\left((\boldsymbol{F}(\boldsymbol{p}) - \boldsymbol{d})_i C_{ij}^{-1}(\boldsymbol{F}(\boldsymbol{p}) - \boldsymbol{d})_j + \lambda^{-2}\boldsymbol{p}_i D_{ij}^{-1}\boldsymbol{p}_i\right)$$

with $V = S^{-1}$, $W = G^{-1}$, $C = SS^T$, $D = GG^T$ (Cholesky factorisation of a p.d. matrix).

Noise levels $\sigma = 0.5, 0.25, 0.1$, $C = \sigma^2 \mathbb{I}$, D approx. with 125 samples.

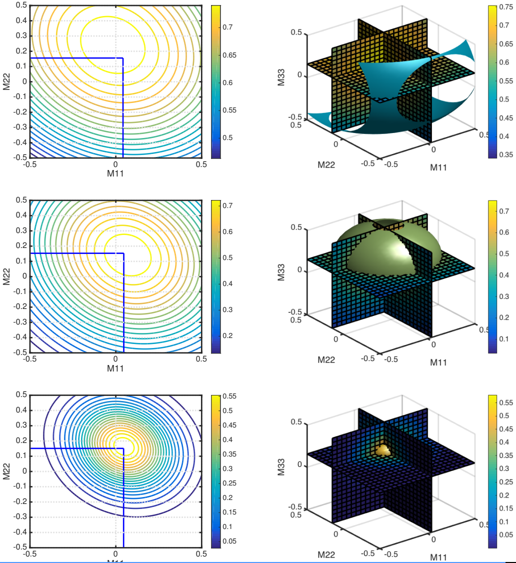

Conclusions

- PS tensor provides the leading order response in EIT and EM scattering, but the situation is different for eddy currents;
- Recent results of Ammari, *et al.* predicts the response in terms of a rank 4 tensor;
- But our recent work shows this does in fact reduce to an expansion involving a symmetric rank 2 tensor $\overset{\smile\smile}{\mathcal{M}}$;
- $\overset{\smile\smile}{\mathcal{M}}$ is part of a family of polarizability tensors for describing the response from conducting and permeable objects;
- Skin effects are important and $\overset{\smile\smile}{\mathcal{M}}$ can be computed by using hp- edge finite elements;
- Asymptotic behaviour of low frequency/high conductivity for $\overset{\smile\smile}{\mathcal{M}}$ investigated where topology plays a role;
- On going work includes developing a Bayesian inverse framework for $\overset{\smile\smile}{\mathcal{M}}$.

References

Thank you

References

- P. D. Ledger, W.R.B. Lionheart, The perturbation of electromagnetic fields at distances that are large compared with the object's size, *IMA Journal of Applied Mathematics*, **80**: 865-892 (2015a).
- P. D. Ledger, W.R.B. Lionheart, Characterising the shape and material properties of hidden targets from magnetic induction data, *IMA Journal of Applied Mathematics*, **80**: 1776-1798 (2015b).
- P.D. Ledger and W.R.B. Lionheart, Understanding the magnetic polarizability tensor, *IEEE Transactions on Magnetics*, **52**, Article # 6201216 (2016).